APPLIED PHYSICS LETTERS VOLUME 85, NUMBER 21 22 NOVEMBER 2004

Interface-oxygen-loss-controlled voltage offsets in epitaxial $Pb(Zr_{0.52}Ti_{0.48})O_3$ thin-film capacitors with $La_{0.7}Sr_{0.3}MnO_3$ electrodes

Wenbin Wu[a]
Structure Research Laboratory, University of Science and Technology of China, Hefei 230026, China, and Department of Applied Physics, The Hong Kong Polytechnic University, Hong Kong, China

K. H. Wong and C. L. Choy
Department of Applied Physics, The Hong Kong Polytechnic University, Hong Kong, China

(Received 1 March 2004; accepted 30 September 2004)

Epitaxial $Pb(Zr_{0.52}Ti_{0.48})O_3$ (PZT) thin-film capacitors with $La_{0.7}Sr_{0.3}MnO_3$ (LSMO) electrodes have been grown on $(LaAlO_3)_{0.3}(SrAl_{0.5}Ta_{0.5}O_3)_{0.7}$ (001) substrates by pulsed-laser deposition. The process-induced imprint behavior in the ferroelectric capacitors was examined by *in situ* and *ex situ* annealing at various conditions. It was found that for the capacitors *in situ* annealed at reduced oxygen pressures, where the LSMO electrodes are stable, voltage offsets in the polarization-electric field hysteresis loops were observed only for those treated at temperatures higher than the Curie temperature. At lower temperatures, the oxygen loss may be suppressed by stresses arising primarily from the paraelectric-to-ferroelectric transformation. However, for the capacitors *ex situ* annealed at the same low temperature, large voltage offsets were induced due to the oxygen instability of the LSMO electrodes. We show evidence that the imprint is caused by oxygen loss at the PZT/LSMO interface, and closely related to the variation of the PZT structure. © *2004 American Institute of Physics*. [DOI: 10.1063/1.1827929]

Among the many families of ferroelectrics, $Pb(Zr,Ti)O_3$ (PZT) and their derivatives have been one of the most extensively studied materials due to their large remnant polarization and low coercive field (E_c). Since PZT capacitors with noble metal electrodes like Pt exhibit a significant polarization loss (fatigue) when subject to bipolar switching pulses, in the past decade, PZT capacitors with oxide electrodes such as $La_{0.5}Sr_{0.5}CoO_3$ (LSCO) have been thoroughly studied.[1–6] For epitaxial LSCO/PZT/LSCO capacitors, however, when exposed to reducing atmosphere for device fabrication, a large voltage offset in the polarization–electric field (P–E) hysteresis loops was observed.[2–5] This process-induced imprint and the mechanism behind it were greatly complicated by the instability of the LSCO electrodes at reduced oxygen pressures.[4,5,7] $La_{0.7}Sr_{0.3}MnO_3$ (LSMO) is also a metallic oxide and when fully oxygenated, epitaxial LSMO films show a room-temperature (RT) resistivity of about 300 μΩ cm, comparable to some other conductive oxide films.[8] Moreover, previous reports have shown that the epitaxial LSMO films are very stable against *in situ* annealing at various oxygen pressures, but unstable when *ex situ* treated at reduced oxygen pressure, which distinguishes them from the LSCO electrodes.[7,9,10] In this letter, we report on the imprint behavior in epitaxial LSMO/PZT/LSMO capacitors. It is demonstrated that the voltage offset is controlled by oxygen loss at the PZT/LSMO interface, and closely related to the change of the PZT structure.

The LSMO and $Pb(Zr_{0.52}Ti_{0.48})O_3$ targets were made by standard solid state reactions. Epitaxial LSMO/PZT/LSMO capacitors were grown on $(LaAlO_3)_{0.3}(SrAl_{0.5}Ta_{0.5}O_3)_{0.7}$ [LSAT(001)] substrates by the pulsed-laser deposition method, as described previously.[11] Both the LSMO and PZT films were grown at 620 °C with the oxygen pressure fixed at 200 mTorr. After deposition, the capacitors were cooled to 550–300 °C in 10 Torr of O_2, and then *in situ* annealed at various reduced oxygen pressure ranging from 10 to 10^{-5} Torr for up to 50 min before being cooled to RT in the same annealing ambient. The as-grown samples were cooled directly to RT in 10 Torr of O_2. Some capacitors were also *ex situ* annealed, i.e., the as-grown or *in situ* annealed samples were further annealed in a different vacuum run with the heating and cooling process conducted in the same atmosphere. The thicknesses of the PZT and LSMO films were about 400 and 150 nm, respectively. The P–E hysteresis loops were measured at RT using a RT66A tester.

Figures 1(a)–1(c) show P–E hysteresis loops measured from the capacitors as-grown and *in situ* annealed at 10^{-3} or 10^{-5} Torr and 550 °C for 30 min, as indicated. The loops become more asymmetric and the corresponding internal bias fields directed toward the top electrode become larger, as the annealing oxygen pressure is reduced further.[3,12] In Fig. 1(c), at a small driving voltage of 2 V, the loop showed no polarization switching due to the large internal field. The imprinted capacitors with P–E loops shown in Figs. 1(b) and

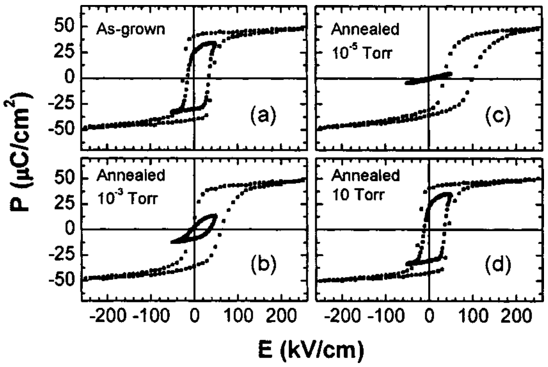

FIG. 1. P–E loops of capacitors as-grown (a), *in situ* annealed in 10^{-3} (b) or 10^{-5} (c) Torr of O_2 for 30 min, and further *ex situ* annealed in 10 Torr of O_2 for 30 min (d). The annealing temperature is 550 °C, and the driving voltage for measuring the P–E loops is 2 and 10 V.

---

[a] Electronic mail: wuwb@ustc.edu.cn

0003-6951/2004/85(21)/5013/3/$22.00

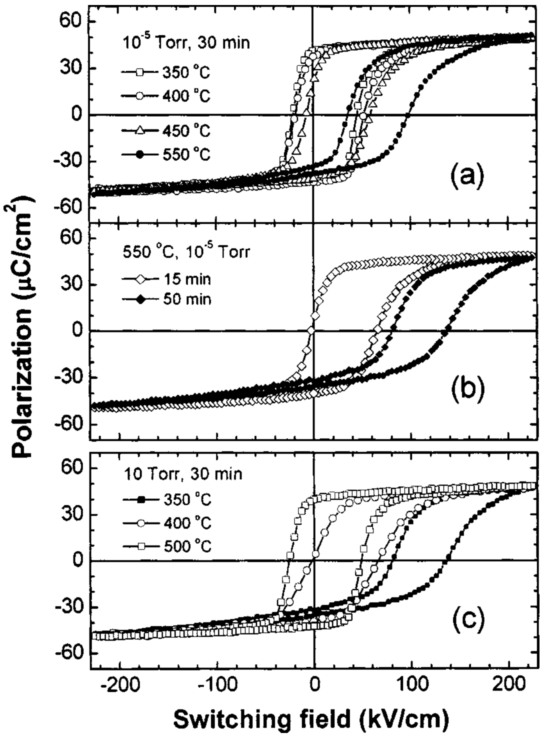

FIG. 2. *P–E* loops of capacitors *in situ* annealed in 10^{-5} Torr at different temperatures (a), and at 550 °C for different times (b). The most imprinted capacitor in (b) was further successively annealed at 350, 400, and 500 °C in 10 Torr, and the loops were recorded in (c). The driving voltage is 9 V.

1(c) were further *ex situ* annealed at 550 °C in 10 Torr of O_2 for 30 min. These capacitors showed almost the same loops as the as-grown capacitors after the *ex situ* oxidizing anneal, as shown in Fig. 1(d), indicating that the formation of the internal field during the *in situ* annealing can be ascribed to oxygen loss from the capacitors.

Figure 2(a) shows *P–E* loops measured from the capacitors *in situ* annealed in 10^{-5} Torr of O_2 for 30 min at 350, 400, 450, and 550 °C, respectively. As the temperature increases, the voltage offsets and the corresponding internal electric fields developed in the annealed capacitors increase. However, compared with the as-grown capacitors [Fig. 1(a)], those treated at temperatures lower than 400 °C showed a quite small internal field. That means at the lower temperatures, the oxygen outdiffusion from the capacitors may be suppressed. At higher temperatures such as 550 °C and in 10^{-5} Torr of O_2, a time evolution to the voltage offsets was also observed [Fig. 2(b)]. For the most imprinted sample an internal field as high as 110 kV/cm, about 4 times of E_c, was recorded, and unlike the LSCO/PZT/LSCO capacitors,[2,4] the reducing annealing has induced a larger voltage offset but slight changes in E_c and the conductivity of the capacitors. This could be attributed to the high thermal stability of the LSMO electrodes under the *in situ* annealing conditions. The loop is also tilting, with the saturated polarization (the asymmetric saturation is due to the upward internal field) almost unchanged at the large driving voltage. This implies that after the reducing anneal there may exist a nonswitching layer possibly at the PZT/LSMO bottom interface,[1] where misfit dislocations and the lattice deformation of PZT layer have been observed previously.[11] To understand more about oxygen diffusion in the system, the most imprinted capacitors were further successively annealed at 350, 400, and 500 °C and 10 Torr for 30 min. According to Fig. 2(c), the annealing at 350 °C has not changed the loop at all, and at higher temperatures the internal field decreases gradually. That means at the lower temperatures, the oxygen indiffusion in the capacitors may also be suppressed.

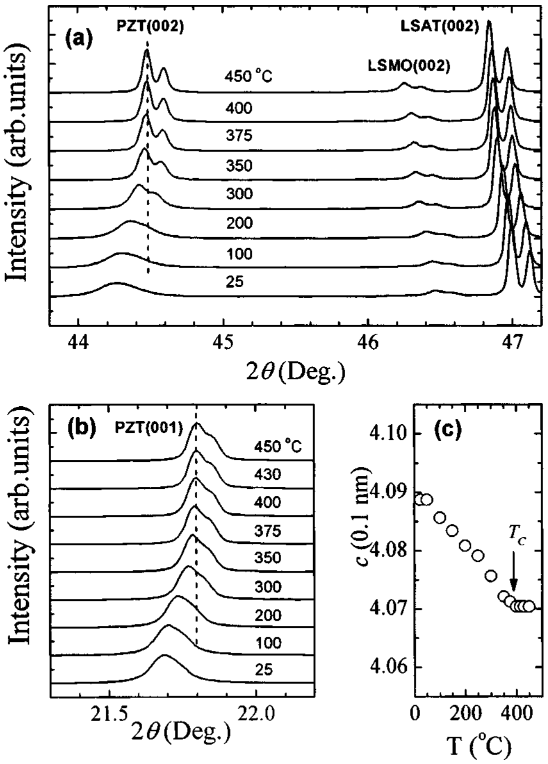

FIG. 3. Temperature-dependent XRD linear scans around the (a) PZT(002) and (b) PZT(001) reflections of an as-grown capacitor. Due to the smaller area (200 μm in diameter and 600 μm in spacing), the reflection from the LSMO top electrode may be too weak to be detected. The dashed line is a guide to eyes for the peak shift. The temperature dependence of the out-of-plane lattice parameter is shown in (c).

After growth and during cooling down, the PZT will transform from the (cubic) paraelectric to (tetragonal) ferroelectric phase. For bulk PZT with a composition similar to that used here for thin films, the Curie temperature (T_C) is 390 °C.[13] To check T_C of the film and to get an insight into the structure evolution during the cooling process, a high temperature x-ray diffraction (XRD) study on the as-grown capacitors was performed. Figure 3(a) shows a set of temperature-dependent XRD θ-2θ scans around (002) reflections of the heterostructure. With increasing temperature, the PZT(002) peak shifts gradually to higher Bragg angles, holding at a fixed position for sample temperatures above 400 °C; its width decreases and at 300 °C it begins to split into Cu $K_{\alpha 1}$ and Cu $K_{\alpha 2}$ reflections. In Fig. 3(b), almost the same changes were observed for the PZT(001) peak, although at the same temperature the split reflections are not well defined due to the low Bragg angles. Figure 3(c) shows variation of the out-of-plane lattice parmeter *c*. These data and features indicate that the T_C of the film is within 375–400 °C.[13–15] It was commonly reported that during deposition and as the film thickness increases (the critical thickness reported is less than 150 nm), the compressive lattice-misfit stresses between PZT and the bottom electrode can be fully relaxed by dislocation generation.[14,16,17] As defects at the PZT bottom interface, these misfit dislocations will form open passages for oxygen diffusion at the high temperatures.[18] As the temperaure decreases, there are no significant thermal stresses de-

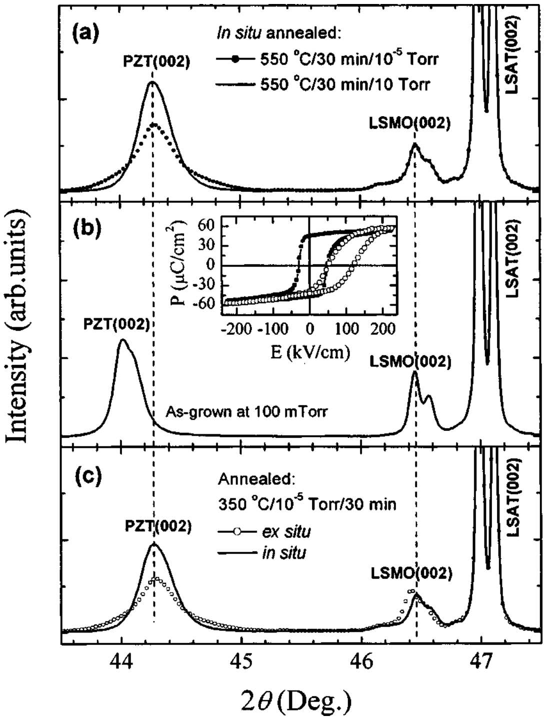

FIG. 4. (a) XRD linear scans from the capacitors *in situ* annealed at 550 °C for 30 min in 10^{-5} (dotted line) or 10 (solid line) Torr of O_2; (b) XRD from an as-grown capacitor with the PZT grown at 100 mTorr of O_2 and the *P-E* loop was recorded in the inset (■). (c) XRD from those *in situ* (solid line) and *ex situ* (dotted line) annealed at 350 °C, 10^{-5} Torr for 30 min. The loop (○) in the inset to (b) is measured from the *ex situ* annealed samples.

veloped, however, at T_C the transformation stresses (tensile) start to increase,[14,16] which is also reflected by the shape change of the PZT(00*l*) ($l=1$ and 2) reflections. We speculate that the internal lattice strains in the PZT films would change the oxygen diffusivity and suppress oxygen diffusion at the lower temperatures, as already mentioned.

Figure 4(a) show RT specular XRD linear scans on the capacitors *in situ* annealed at 550 °C in 10^{-5} or 10 Torr of O_2 for 30 min. The profiles confirmed that the LSMO electrode is stable against the *in situ* annealing at various oxygen pressures, since the same LSMO(002) reflections were recorded. On the other hand, it is seen that with the large voltage offset observed [Fig. 1(c)], the capacitors after the 10^{-5}Torr *in situ* anneal showed a depressed PZT(002) reflection with a much larger width. However, the peak position has not changed, suggesting that the imprint was not induced by oxygen loss in the bulk of the PZT film. For perovskite oxides, an increase of oxygen vacancies in the film could usually result in an increase of the out-of-plane lattice constant.[10,19] Based on this consideration, as-grown capacitors with the PZT layer (400 nm thick) deposited at a lower oxygen pressure of 100 mTorr were fabricated. As shown in Fig.4(b), with the oxygen content decreased, the PZT(002) peak shifts to a lower Bragg angle, as expected. But, no large voltage offset was observed for the oxygen deficient PZT film [inset in Fig. 4(b), filled squares]. This also suggests that the imprint was not induced by oxygen loss in the bulk of the PZT film. Figure 4(c) shows XRD linear scans on the capacitors *in situ* and *ex situ* annealed at a low temperature of 350 °C in 10^{-5} of O_2 for 30 min. For the *in situ* annealed samples, both the LSMO and PZT layers are stable, and no voltage offset was observed [Fig. 2(a)]. For the *ex situ* annealed samples, since the LSMO electrode is unstable in this process, as reflected by the small peak shift of LSMO(002), an oxygen loss at the PZT/LSMO interface has been induced at the same low temperature, and as such, a large voltage shift occurred for the *ex situ* annealed capacitors [inset in Fig. 4(b), unfilled circles]. That means the imprint could be induced by oxygen loss at the PZT/LSMO interface. It should be noted that we measured a similar change in the shape of PZT(002) reflection after the 350 °C *ex situ* anneal as was observed subsequent to the 550 °C *in situ* anneal. Thus, our results demonstrated that the process-induced imprint is controlled by oxygen loss at the PZT/LSMO interface, and closely related to the variation of the PZT structure. Stresses at interfaces and the thermal stability of the constituent layers could affect oxygen diffusion, and so the imprint. At present, the broadening of the PZT(002) reflection due to the reducing annealing could be understood as a manifestation of the interface-oxygen-loss-induced large scale strain gradient along the growth direction,[12,14] but the annealing effects on polydomain formation in the PZT films and the interplay between the different strains are still open questions.

This work was supported by the Chinese Natural Science Foundation, the Ministry of Science and Technology of China, and the The Hong Kong Polytechnic University.

[1] J. F. M. Cillessen, M. W. J. Prins, and R. M. Wolf, J. Appl. Phys. **81**, 2777 (1997).

[2] G. E. Pike, W. L. Warren, D. Dimos, B. A. Tuttle, R. Ramesh, J. Lee, V. G. Karamidas, and J. T. Evans, Jr., Appl. Phys. Lett. **66**, 484 (1995).

[3] J. Lee, R. Ramesh, V. G. Keramidas, W. L. Warren, G. E. Pike, and J. T. Evans, Jr., Appl. Phys. Lett. **66**, 1337 (1995).

[4] S. Aggarwal, A. M. Dhote, R. Ramesh, W. L. Warren, G. E. Pike, D. Dimos, M. V. Raymond, and J. T. Evans, Jr., Appl. Phys. Lett. **69**, 2540 (1996).

[5] T. Friessnegg, S. Aggarwal, R. Ramesh, B. Nielsen, E. H. Poindexter, and D. J. Keeble, Appl. Phys. Lett. **77**, 127 (2001).

[6] S. H. Kim, D. J. Kim, J. Hong, S. K. Streiffer, and A. I. Kingon, J. Mater. Res. **14**, 1371 (1999).

[7] S. Madhukar, S. Aggarwal, A. D. Dhote, R. Ramesh, A. Kishnan, D. Keeble, and E. Poindexter, J. Appl. Phys. **81**, 3543 (1997).

[8] J. M. D. Coey, M. Viret, L. Ranno, and K. Ounadjela, Phys. Rev. Lett. **75**, 3910 (1995).

[9] W. Wu, K. H. Wong, X.-G. Li, C. L. Choy, and Y. H. Zhang, J. Appl. Phys. **87**, 3006 (2000).

[10] J. R. Sun, C. F. Yeung, K. Zhao, L. Z. Zhou, C. H. Leung, H. K. Wong, and B. G. Shen, Appl. Phys. Lett. **76**, 1164 (2000).

[11] W. Wu, K. H. Wong, C. L. Choy, and Y. H. Zhang, Appl. Phys. Lett. **77**, 3441 (2000); W. Wu, Y. Wang, G. K. H. Pang, K. H. Wong, and C. L. Choy, *ibid.* **85**, 1583 (2004).

[12] A. Gruverman, B. J. Rodriguez, A. I. Kingon, R. J. Nemanich, A. K. Tagantsev, J. S. Cross, and M. Tsukada, Appl. Phys. Lett. **83**, 728 (2003).

[13] B. Noheda, J. A. Gonzalo, L. E. Cross, R. Guo, S.-E. Park, D. E. Cox, and G. Shirane, Phys. Rev. B **61**, 8687 (2000).

[14] Y. M. Kang and S. Baik, J. Appl. Phys. **82**, 2532 (1997); K. S. Lee and S. Baik, *ibid.* **85**, 1995 (1999); **87**, 8035 (2000).

[15] S. K. Streiffer, J. A. Eastman, D. D. Fong, C. Thompson, A. Munkholm, M. V. Ramana Murty, O. Auciello, G. B. Bai, and G. B. Stephenson, Phys. Rev. Lett. **89**, 067601 (2002).

[16] A. L. Roytburd, S. P. Alpay, L. A. Bendersky, V. Nagarajan, and R. Ramesh, J. Appl. Phys. **89**, 553 (2001).

[17] C. M. Foster, Z. Li, M. Buckett, D. Miller, P. M. Baldo, L. E. Rehn, G. R. Bai, D. Guo, H. You, and K. L. Merkle, J. Appl. Phys. **78**, 2607 (1995).

[18] C. Kittel, *Introduction to Solid State Physics*, 6th ed. (John Wiley, Singapore, 1988).

[19] E. J. Tarsa, E. A. Hachfeld, F. T. Quinlan, J. S. Speck, and M. Eddy, Appl. Phys. Lett. **68**, 490 (1996).